AIAA-2001-0414

QUANTITATIVE ACETONE PLIF IN TWO-PHASE FLOWS

B. D. Ritchie* and J. M. Seitzman†

Georgia Institute of Technology
Aerospace Combustion Laboratory
School of Aerospace Engineering
Atlanta, GA 30332-0150

Abstract

A model for fluorescence signal extinction due to an acetone droplet is developed. When combined with existing models, it provides a system of two equations in two unknowns for the fluorescence and extinction in a pixel in two-phase flow. The model is used to define parameters necessary for sufficient resolution in an acetone PLIF experiment. It can also be used to convert acetone PLIF images into images of droplet location and size as well as local vapor concentration. Approximation methods to achieve this conversion are discussed. The qualitative effects expected based on the model are shown in experimental results.

Introduction

Quantitative two-phase mixture fraction measurements are important for understanding mixing in two-phase systems typical of modern combustion systems. This understanding can lead to the reduction of pollutants, improved combustor efficiency, reduced combustor size, longer combustor lifetimes and greater combustor stability. Thus there is a great need for the development of appropriate measurement techniques. This study focuses on developing quantitative, spatially and temporally resolved measurements in two-phase flow using planar laser-induced fluorescence (PLIF) of acetone to measure both liquid and vapor concentrations with one technique.

Planar laser-induced fluorescence (PLIF) is well suited to the task of measuring mixing because it yields two-dimensional images of the flowfield and is a proven approach for non-invasive measurements.[1] A laser beam at a properly chosen wavelength is optically converted to a thin laser sheet that causes molecules in the flowfield to fluoresce. The resulting fluorescence is proportional to the amount of the absorbing species in the measurement volume. The concentration field of the absorber can be converted to mixture fraction, a measure of local mixing.

For fuel-air mixing measurements, acetone fluorescence is especially attractive.[2] It has many advantages over other fluorescing alternatives. Most importantly, acetone fluorescence in isobaric, isothermal flows is known to be linear with concentration and laser power,[3] which is not true for many fluorescing molecules. Additionally, acetone fluorescence works well in the presence of oxygen.

The fluorescence yield of acetone is limited by rapid intersystem crossing from the first excited singlet state (S1), which fluoresces, to the first excited triplet state (T1), which phosphoresces. The phosphorescence is strongly quenched by oxygen, leaving a strong fluorescence signal. Also, acetone absorbs ultraviolet light (225 - 320 nm) but fluoresces in the blue[3] (350 - 550 nm). Elastically scattered light is easily filtered out by simple glass optics since the absorption and emission spectra do not overlap.

Using pure acetone instead of doping another liquid reduces experimental complexity. A further advantage of using pure acetone as the liquid is that the high vapor pressure makes it simple to recreate the high evaporation rates of fuel sprays in engines without elaborate heating systems. Finally, acetone is much

* Graduate Student, Student Member AIAA
† Associate Professor, Senior Member AIAA

Copyright © 2001 by B. Ritchie.
Published by the American Institute of Aeronautics and Astronautics, Inc. with permission.

less toxic than many alternative molecules. Although prolonged exposure should be avoided, breathing small amounts of acetone vapor does not present a serious health risk.

In this study, mixing between an annular air jet and a conical acetone spray is affected with zero net-mass-flux actuators known as synthetic jets. These synthetic jets cause momentum transfer by taking in fluid from all directions and outputting fluid in a well-directed and high velocity jet. The devices used here operate at a frequency close to 1.2 kHz. Since they use the local fluid, they require no external plumbing. Electronic control of these actuators allows implementation of different control strategies without physical changes to the device. Velocity measurements[4] show that these high-frequency actuators excite small scales in the flow.

Experimental Apparatus and Procedure

Flow Facility

Two vertical coaxial jets are formed by a central hole in a metal body (which houses the synthetic jet actuators), a concentric tube and a spray nozzle inside the inner tube (see Figure 1). The outside exit diameter (D_o) is 2.54 cm, the inner tube has an inner diameter (D_i) of 1.41 cm and a wall thickness (t) of 0.9 mm, and the spray nozzle is 1.11 cm in diameter. The outer annular flow moves at a mean exit velocity of 6 m/s while the inner flow has a mean exit velocity of 6 or 12 m/s depending on the test. Both flows are fully developed due to the length of the tubing from the flow source to the exit.

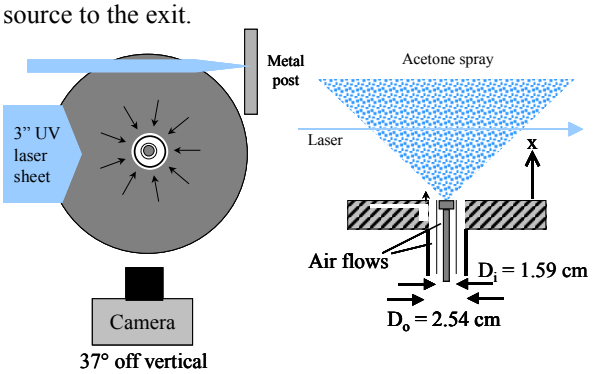

Figure 1. Two schematics of the experimental setup. On the left is a view from above the experiment while a side view is shown on the right.

The nozzle is a Hago M5 precision mini nozzle, which generates a solid cone spray of 3.16 gph at 40 psig with a Sauter Mean Diameter of 45.2 µm. The exits of the nozzle and the inner tube are coplanar with the top of the metal body. The metal body houses nine synthetic jet actuators equally spaced around the circumference of the coaxial jets. Each jet orifice is an arc 0.5 mm wide and 9 mm long. The synthetic jets are directed parallel to the coaxial jets (Figure 1). The actuators are located near the exit plane to enhance mixing of the central flows and the surrounding air.

The synthetic jets are created by synthesis of the periodic flow caused by alternating suction and blowing through the actuator orifice driven by the oscillations of an internal membrane at or near its resonance frequency. The actuators are driven at 1.18 kHz in these experiments by a common signal source. However, each actuator is driven by a dedicated amplifier set so that every actuator provides approximately a 10 m/s synthetic jet at x/h = 12.5 (x/D_o = 0.25).

Imaging Setup

The imaging setup employs a frequency-quadrupled Nd:YAG laser (266 nm) beam. The 7 mm circular output beam of the Nd:YAG laser is converted into a 170 µm tall collimated sheet that is 80 mm wide. The sheet is produced with one spherical lens to reduce the sheet thickness and a telescope consisting of two cylindrical lenses to provide the sheet width. The laser energy is approximately 100 mJ per pulse and the temporal full-width at half-maximum value of the pulse is 7 ns.

The image is acquired by a 1024×1024 pixel, CCD camera with ~70% quantum efficiency in the wavelength range of acetone fluorescence and a 50 mm f/1.8 glass photographic camera lens. A holographic notch filter for frequency-doubled Nd:YAG light (532 nm) is placed in front of the lens to reject scattered residual 532 nm light in the laser sheet. The camera employs a thinned, back-illuminated, UVAR coated, and Peltier-cooled CCD, which provides low light level sensitivity and a large signal dynamic range.

The camera is held 37° off vertical to prevent acetone from hitting the camera or lens. The excellent spatial resolution of the system is important since the acetone concentration measurements can only be interpreted as molecular mixing measurements if the images are spatially resolved on the order of the Kolmogorov scale.[5] Full jet cross-section images are acquired at multiple downstream locations (x/D_o = 1,5,10) for comparison purposes between images covering the range from having many droplets but little vapor near the exit to having a lot of vapor and few droplets farther downstream.

Image Correction

The measured fluorescence signal from each pixel of the camera is a function of a number of experimental

parameters in addition to the acetone concentration. Thus the PLIF images must be corrected before being interpreted as quantitative measurements.[6] First, the background signal from ambient light and any fluorescence or phosphorescence from the experimental setup itself due to the laser (e.g., fluorescence from the metal body) must be subtracted. The laser sheet does not have a uniform intensity along its width, and thus a sheet intensity correction is required.

The data must also be corrected for the shot-to-shot fluctuation in laser energy. To make this correction, the reflection from the front surface of the first lens is used to make a second, small and low energy laser sheet that hits a metal post and the combined fluorescence and phosphorescence is imaged. This signal is a function of the shot-to-shot laser energy.

Once the images have been corrected for these temporal and spatial effects, the images must adjusted to account for absorption of the laser by acetone vapor and acetone droplets. The final result is an image of the spatially resolved acetone vapor number density, and effective droplet diameters.

Model

A key to making quantitative LIF measurements in multiphase flows is distinguishing between the signal coming from different phases. Droplets sufficiently larger than a pixel can be resolved geometrically. Thus phase discrimination is primarily an issue for subpixel sized droplets. Since both phases of acetone fluoresce over essentially the same spectrum,[7] the phases cannot be readily distinguished spectrally.

However, the large density difference between the phases leads to a solution. The higher density of liquid acetone (~750× the vapor density at standard conditions) leads to much larger signals from droplets compared to vapor of the same volume. Thus, signal strength can be used to separate liquid from vapor acetone, but only for droplets larger than some minimum critical diameter. The reason is the very short optical depth (≈18 μm)[7] of liquid acetone for ultraviolet wavelengths. For particle diameters somewhat larger than the optical depth, the liquid in the droplet beyond the optical depth does not contribute to the fluorescence signal, as the laser intensity becomes neglible.

The liquid absorption also impacts acetone LIF measurements of the vapor phase. Since the strong absorption limits the maximum signal from large droplets, the dynamic range of the camera required to view both droplets and low vapor concentrations is reduced. Behind large enough droplets, there will also be laser "shadow", preventing measurement of the acetone vapor downstream of the droplet. This limits the usefulness of two-phase acetone imaging in dense spray regions.

In preparation for two-phase experiments, a model is needed for distinguishing between the fluorescence from droplets and that from vapor. Calculations to determine the cutoff diameter for distinguishing the two phases are necessary to make sure that droplet diameters of interest can be measured. One example is validation of a complex computational fluid dynamics code that predicts evaporation and mixing. Such codes track droplets to some minimum diameter and then assume the droplet evaporates instantly. Experiments that only distinguish down to 100 μm droplet diameters are little help if the code tracks them down to 5 μm in diameter.

A simple model to account for droplet fluorescence has been given for a spherical droplet with an index of refraction that matches the vapor value.[7] This choice of refractive index eliminates reflection and refraction at the surface. The model was also derived for a top hat laser profile, with the droplet always entirely inside the sheet, and square camera pixels. In this case, the fluorescence is given by:

$$S_d \equiv \eta / 2 \, I_0 \pi d^2 [1-\exp(-Kd/3)] \qquad (1)$$

where d is the droplet diameter, K is the absorption coefficient, and η is the fluorescence efficiency.

This approximation shows that the fluorescence is proportional to volume for small droplets ($Kd/3 << 1$) while it scales like surface area for large droplets. Experimental results do not fit this model, however. Acetone has an index of refraction of 1.36, resulting in reflection and refraction at the droplet surface. A modified model, that reduces to the original for n = 1, was proposed[7] to account for this, and is given by:

$$S_d \equiv \eta / 2 \, I_0 \pi d^{(3-n)} [1-\exp(-Kd^n/3)] \qquad (2)$$

It was found that an index of refraction (n) of 1.43 best fit the data. Potentially this could be a dispersion effect resulting from aspherical droplets. Using Equation 2 to model droplet signal, results have been presented in previous work.[8] This work calculated the equivalent size of a pixel full of a homogeneous mixture of acetone vapor and air needed to generate the same fluorescence power as a droplet of pure acetone.

The current model still assumes spherical droplets, but improves on the modeling of reflection and refraction effects. Instead of keeping a form that reduces to the ideal droplet model like Equation 2, the current model uses more correct computations based on basic light scattering principles for small droplets.[9] Several assumptions are inherent in the model. All liquid acetone within the volume imaged in a pixel is treated as one droplet, since there is no way to tell the number of droplets from the total amount of signal. This means multiple small droplets would be combined into one larger droplet, and droplets that are split between pixels would be treated as two separate

droplets of smaller size while any part of a droplet outside of the imaging volume would be ignored. Within each pixel volume, the gas mixture is assumed to be homogeneous and not to cause scattering.

The current model results in the following four equations. The pixel extinction coefficient due to a droplet only (PEC_d), where extinction is composed of scattering and absorption, given by:

$$PEC_d = \pi(d/2t)^2[1.045\text{-}0.923\exp(\text{-}0.42456dK_d)] \quad (3)$$

where d is the droplet diameter, t is the laser sheet thickness and K_d is the absorption coefficient. This represents a 7.7% loss of light to the next pixel due to reflection and a 12.2% loss due to scattering out of the plane. The mean path length through the droplet is 0.42456d.

For practical purposes, it is easier to work with the normalized fluorescence signal given from a droplet than the absolute value. Thus, Equation 2 becomes:

$$S_d/I_0 = \pi d^{3-n}[1\text{-}\exp(\text{-}K_d d^n/3)]/2 * (t/t_{ref})^2 \quad (4)$$

Where t_{ref} is a reference sheet thickness used to maintain constant energy in the laser sheet instead of a constant intensity as the sheet thickness changes. In the case of acetone vapor, the scattering due to acetone molecules is ignored. This results in a pixel extinction coefficient due to vapor only (PEC_v), where extinction is only due to absorption, given by:

$$PEC_v = 1\text{-}\exp(\text{-}\sigma_v N_v t) \quad (5)$$

where σ_v is the absorption cross-section of acetone vapor, and N_v is the number density of acetone vapor. The normalized fluorescence signal from the acetone vapor in the pixel is given by:

$$S_v/I_0 = \sigma_v N_v t^3 * (t/t_{ref})^2 \quad . \quad (6)$$

Equations 3 and 5 can be combined to give the total pixel extinction coefficient:

$$PEC = \pi(d/2t)^2[1.045\text{-}0.923\exp(\text{-}0.42456dK_d)] + 1\text{-}\exp(\text{-}\sigma_v N_v t) \quad (7)$$

which has only two variables, droplet diameter and acetone vapor number density. K_d and σ_v are physical constants for an isobaric and isothermal system and a known wavelength, while t is determined by the optics that create the laser sheet. Similarly, Equations 4 and 6 can be combined into Equation 8 for the total normalized fluorescence signal from a pixel, given by:

$$S/I_0 = \pi d^{3-n}[1\text{-}\exp(\text{-}K_d d^n/3)]/2 + \sigma_v N_v t^3 \quad (8)$$

which also has just droplet diameter and acetone vapor number density as variables. The model allows data analysis routines to use the signal and the extinction from the pixel to determine the combination of droplets and vapor based on two equations (Equations 7 and 8) in two unknowns (d and N_v).

Using this model, we can compare the fluorescence signal from a droplet (Equation 4) to the fluorescence signal from vapor (Equation 6). The model calculates the length of one side of the pixel filled only with gas that is necessary to generate the same amount of fluorescence as a droplet of a given size using:

$$\text{pixel size} = [(\rho_d/\rho_v) / (Kf_v)*(S_d / I_0)*(t/t_0)^2]^{1/3} \quad (9)$$

The density ratio between liquid and pure vapor, ρ_d/ρ_v, is known for a given temperature. The mole fraction of acetone vapor, f_v, can be chosen as any attainable value for that temperature. S_d/I_0 is calculated with Equation 4 for a given droplet diameter.

Results

The results shown in Figure 2 are the calculations of the fluorescence signal and pixel extinction coefficient generated by an acetone droplet as a function of droplet diameter for three sheet thicknesses: 150 µm, 170 µm and 200 µm. This figure enables relates the expected signal or pixel extinction coefficent to a known droplet diameter. Alternatively, it allows the computation of the droplet diameter based on either the fluorescence signal or the pixel extinction coefficient. Small errors in the sheet thickness translate into a large error in droplet size, especially for larger droplets. Small droplets cause very little extinction, so signal strength is the better parameter to use to calculate the droplet diameter.

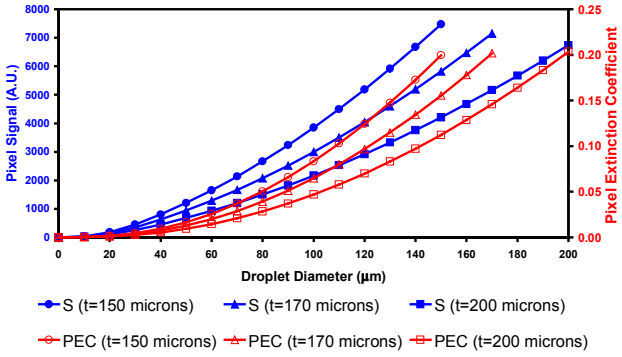

Figure 2. Fluorescence signal and pixel extinction coefficient versus droplet diameter for liquid acetone, for three sheet thicknesses: 150 µm (●), 170 µm (▲) and 200 µm (■).

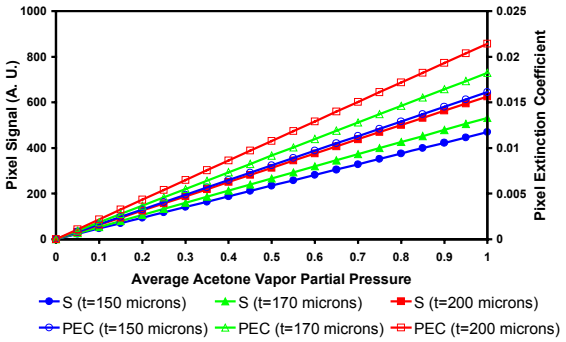

Figure 3. Fluorescence signal versus the acetone vapor partial pressure, for three sheet thicknesses: 150 µm (●), 170 µm (▲) and 200 µm (■). Also, pixel extinction coefficient versus the acetone vapor partial pressure, for the same sheet thicknesses: 150 µm (○), 170 µm (△) and 200 µm (□).

The next results (Figure 3) show the fluorescence signal and pixel extinction coefficient by a volume of an acetone-air mixture for cubic pixels the size of the sheet thickness for the same three pixel sizes. At room temperature, the partial pressure of acetone is about 30%. The signal scales linearly with the concentration of acetone and also with the cube of the sheet thickness since that defines the acetone volume. The pixel extinction coefficient scales almost the same way because the the exponent is so small in the exponential function that it can be approximated as linear by only using two terms of the Taylor series expansion.

The next set of results focuses on the fluorescence signal. Room temperature is used to determine the density ratio between the two phases as well as the saturation concentration of acetone. When combined on one plot (Figure 4), it is easy to compare the signals from the two phases. This plot allows calculation of either the minimum vapor concentration or the maximum droplet size measurable if both the other value and the dynamic range of the imaging system are known. The air is saturated with acetone vapor for the results presented here. As expected, small droplets have a signal that scales with volume while the vapor signal scales with area (pixel size squared) with a constant sheet thickness.

One goal of this model is to calculate the equivalent pixel size for a given droplet diameter, allowing *a priori* knowledge of the resolution required for a given field of view before an experiment is designed. There are two values held constant in the model that have a significant impact on the results. The equivalent pixel size scales inversely with the thickness of the laser sheet (Figure 5). This can be determined from Equation 9, which shows that the incident intensity scales like 1/t. The mole fraction of acetone vapor in the volume imaged onto the pixel is also important (Figure 6). From Equation 9, the equivalent pixel size scales like one over the cube root of the mole fraction.

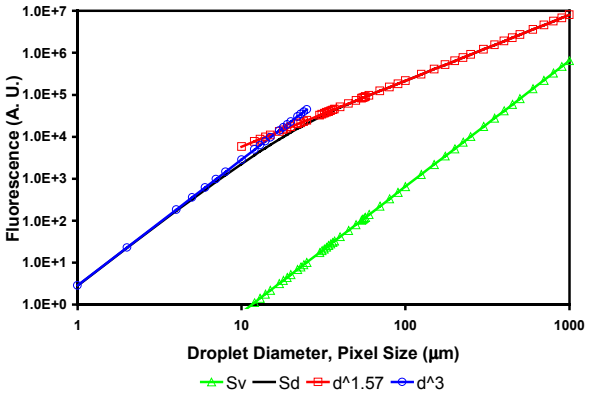

Figure 4. Fluorescence power versus droplet diameter for liquid acetone and versus pixel size for saturated vapor at room temperature. Fluorescence power scales like d^3 for small droplets and like d^{3-n} for large droplets.

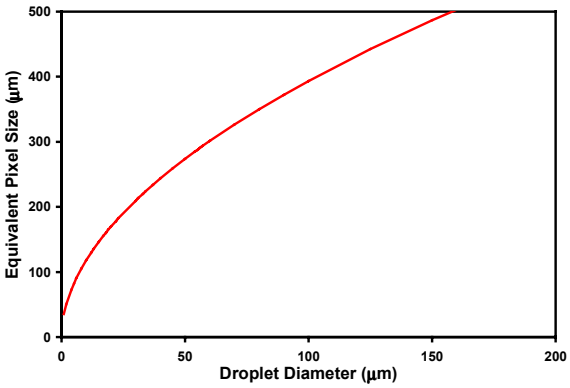

Figure 5. Equivalent pixel size to emit the same fluorescence power, assuming saturated vapor, for a given droplet size.

The model results in a cutoff diameter of ~ 20 µm for the experimental conditions, at which an entire pixel of saturated acetone vapor would produce the same signal as the droplet. This cutoff size is dependent on the pixel size and the ambient conditions. A smaller pixel can contain less vapor while a lower temperature will reduce the vapor pressure of acetone and thus the saturation level of vapor. Both of these conditions would decrease the cutoff diameter.

The solution to this is to approximate by only using the signal strength. One way is to calibrate the PLIF using a scattering technique. Once a correlation is found between signal strength and droplet size, this can be used to analyze future data. If a calibration is not possible, a less accurate approximation can be used. Signal levels above a certain value can be treated as coming entirely from liquid acetone. This introduces

an error, but for a cutoff sized droplet of 20 µm in a 170 µm ^3 of saturated vapor at 25 °C the equivalent droplet would be 27 µm in diamter. The percentage of maximum error drops quickly as the droplet diameter increases and as the vapor concentration decreases, but increases quickly with temperature. Conversely, all pixels with signals below the cutoff can be treated as vapor, which introduces the opposite error. This method is best suited to a flowfield with a small number of droplets expected. A global check on the data analysis can be done by providing a reference flow on the trailing end of each image. The results will be correct only if the cumulative pixel extinction is correct. Too much acetone being treated as droplets will lead to overestimating the extinction due to reflection and refraction losses. If the flow is symmetric, a comparison between the two sides can check the accuracy of the results.

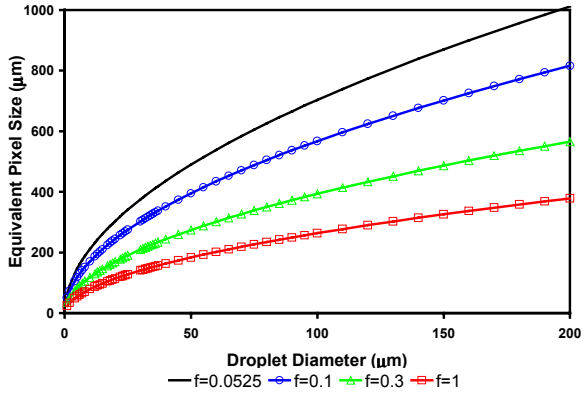

Figure 6. Equivalent pixel size to match the fluorescence power generated by a droplet of a certain size for different mole fractions of acetone vapor.

Figure 7 shows a plot of the fluorescence signal values for a row of pixels in the direction of laser propagation across an acetone PLIF image taken 10 diameters downstream. The lower line is not corrected for extinction due to acetone molecules, and the higher one is. The expected effects are demonstrated qualitatively by the large spike caused by a sizeable droplet (70 µm) and the smaller spike due to a smaller droplet (40 µm). These droplet sizes agree with the model prediction for both signal and extinction, and provide the proper correction as evidenced by the plateau region of saturated vapor. The steady decrease in the signal across the region of saturated vapor is evidence of the extinction effect gradually decreasing the laser intensity and thus reducing the signal. The same effects are seen nearer the exit, but with many more droplets and less vapor making it more difficult to notice the effects by eye. The images qualitatively show the expected results. Droplets are very noticeable, but the spray never contained any droplet large enough to completely shadow the acetone past it from the laser.

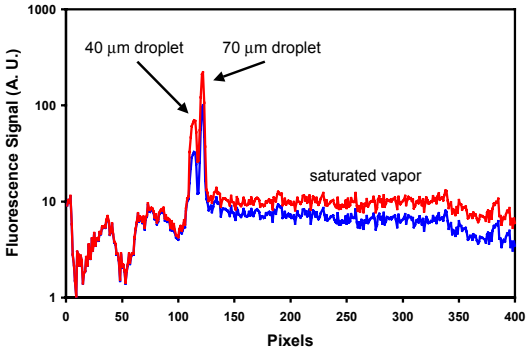

Figure 7. Fluorescence signal values, uncorrected (lower) and corrected (higher) for the extinction due to acetone, for a row of pixels in the direction of laser propagation from an acetone PLIF image taken ten diameters downstream. Peaks corresponding to two droplets are indicated.

Conclusions

A model for the extinction due to acetone droplets has been developed. It has been combined with models for the fluorescence signal from an acetone droplet, the fluorescence from acetone vapor, and the absorption by acetone vapor. When combined, these models reduce to a system of two equations (total fluorescence signal and total pixel extinction) in two unknowns (droplet diameter and vapor number density).

The effects on discriminating droplets from vapor based on fluorescence signal from changing the pixel size and of having different acetone vapor concentrations are discussed. Clearly the ideal case is to have small pixels and a low temperature, which both reduce the amount of acetone vapor in a pixel and thus decrease the cutoff for droplet discrimination. This model allows the user to calaculate *a priori* the resolution needed in a PLIF experiment to discriminate liquid droplets of the minimum size of interest from vapor based on just PLIF images. Used in reverse, the model can correct PLIF images into images of the actual location of droplets, including their sizes, as well as the local acetone vapor.

Getting exact results is complicated by the difficulty in finding accurate values for the pixel extinction based on PLIF data. Several methods of approximation are discussed, and the best choice depends on the necessary accuracy. Qualitiative PLIF images show that the technique is viable in a spray. The expected effects of strong droplet signals and gradual signal decay in vapor due to absorption are

shown. The practicality of the technique is shown by never having a droplet shadow the rest of the acetone from the laser.

Acknowledgments

This work was sponsored by the Army Research Office under a Multidisciplinary University Research Initiative program with Dr. David Mann as technical monitor.

References

[1]Seitzman, J. M. and Hanson, R. K., "Planar Fluorescence Imaging in Gases," Chapter 6 in Instrumentation for Flows with Combustion, ed. A. M. K. P. Taylor, Academic Press, London, (1993).

[2]Lozano, A., Smith, S. H., Mungal, M. G. and Hanson, R. K., "Concentration Measurements in a Transverse Jet by Planar Laser-Induced Fluorescence of Acetone," AIAA Journal **32**, 218-221, (1994).

[3]Lozano, A., Yip, B. and Hanson, R. K., "Acetone: A tracer for concentration measurements in gaseous flows by planar laser-induced fluorescence," Experiments in Fluids **13**, 369-376, (1992).

[4]Davis, S. A. and Glezer, A., "The Manipulation of Large- and Small-Scales in Coaxial Jets using Synthetic Jet Actuators," AIAA Paper 2000-0403, 38th Aerospace Sciences Meeting, Reno, NV, 2000.

[5]Broadwell, J. E. and Mungal, M. G., "Large Scale Structures and Molecular Mixing," Physics Fluids A **3**, 1193-1206, (1991).

[6]Ritchie, B. D. and Seitzman, J. M., "Controlled Fuel-Air Mixing Using a Synthetic Jet Array," AIAA Paper 2000-3465, 36th AIAA/ASME/SAE/ASEE Joint Propulsion Conference, Huntsville, AL, 2000.

[7]Bazile, R. and Stepowski, D., "Measurements of Vaporized and Liquid Fuel Concentration in a Burning Spray Jet of Acetone Using Planar Laser Induced Fluorescence," Experiments in Fluids **20**, 1-9, (1995).

[8]Ritchie, B. and Seitzman, J. M., "Acetone Imaging for Measurement of Enhanced Mixing from a Fuel Injector," AIAA Paper 97-2380, 28th Plasmadynamics and Lasers Conference, Atlanta, GA, 1997.

[9] Van de Hulst, H. C., Light Scattering by Small Particles, Dover Publications, Inc., New York, (1981).